journal

J. Am. Ceram. Soc., 97 [2] 420–426 (2014)
DOI: 10.1111/jace.12721

$Pb(Mg_{1/3}Nb_{2/3})O_3$–$PbTiO_3$ Textured Ceramics with High Piezoelectric Response by a Novel Templated Grain Growth Approach

Harvey Amorín,[‡,†] Hana Uršič,[§] Pablo Ramos,[¶] Janez Holc,[§] Rodrigo Moreno,[‖] Daniel Chateigner,[††] Jesús Ricote,[‡] and Miguel Algueró[‡]

[‡]Instituto de Ciencia de Materiales de Madrid, CSIC, Cantoblanco, Madrid 28049, Spain

[§]Jozef Stefan Institute, Jamova 39, Ljubljana 1000, Slovenia

[¶]Universidad de Alcalá, Alcalá de Henares 28871, Spain

[‖]Instituto de Cerámica y Vidrio (ICV), CSIC, Cantoblanco, Madrid 28049, Spain

[††]UMR 6508 CRISMAT Laboratory, ENSICAEN/CNRS, IUT-Caen, Université de Caen-Basse Normandie, Caen F-14050, France

$Pb(Mg_{1/3}Nb_{2/3})O_3$–$PbTiO_3$ is used as a model system of perovskite solid solutions with very high piezoelectric response at tailored morphotropic phase boundaries to demonstrate the processing of textured ceramics by ceramic-only technology. A novel homogeneous templated grain growth approach that uses conventional ceramic procedures and a single-source nanocrystalline powder for the matrix and also for obtaining the templates is described. Two batches of (100) faceted cube-shaped microcrystals with average sizes of 27 and 10 μm were successfully used as templates, and aligned by tape casting for the processing of <001>-textured $Pb(Mg_{1/3}Nb_{2/3})O_3$–$PbTiO_3$ piezoelectric ceramics. Materials with effective piezoelectric coefficients up to 1000 pC/N and ferroelectric properties approaching those of single crystals are obtained.

I. Introduction

Ceramic texturing of ferroelectric perovskite oxides is the key to the development of novel high-sensitivity piezoelectrics technologies, such as energy harvesters[1,2] and composite magnetoelectric devices.[3,4] It must also enable enhanced sensitivity and power in mature technologies such as sensors, actuators, smart systems, underwater acoustics, and ultrasound generation and sensing for nondestructive testing and medical applications.[5]

Efforts are concentrated in perovskite solid solutions with specific ferroelectric morphotropic phase boundaries in their phase diagram (MPBs), for materials at these phase instabilities show the highest known piezoelectric coefficients.[6] This is the case of $Pb(Zr,Ti)O_3$ (PZT), on which commercial high-sensitivity piezoelectric ceramics are based. Large piezoelectric activity is obtained at the MPB between rhombohedral *R*3*m* and tetragonal *P*4*mm* polymorphs, associated with the existence of an intermediate monoclinic *Cm* phase,[7] and of an enhanced transverse dielectric permittivity and thus, shear piezoelectric coefficient at the phase boundaries.[6] This mechanism for high piezoelectricity that involves the rotation of the spontaneous polarization[8] is the same one responsible of the ultrahigh piezoelectric response of $Pb(Zn_{1/3}Nb_{2/3})O_3$–$PbTiO_3$ and $Pb(Mg_{1/3}Nb_{2/3})O_3$–$PbTiO_3$ single crystals along the <100> direction.[9] These crystals can show effective d_{33} piezoelectric coefficients exceeding 2500 pC/N that has to be compared with about 600 pC/N for soft (chemically engineered) PZT piezoelectric ceramics.[10]

Nevertheless, and though commercial ultrahigh piezoelectric crystals are already available, and ongoing research is intensive,[11] crystal growth is complex and time-consuming (typically several days), and crystals are fragile, so a major challenge is the processing of textured ceramics with properties approaching those of single crystals.

In 2001, a pioneering work reported the successful processing of <001>-oriented $Pb(Mg_{1/3}Nb_{2/3})O_3$–$PbTiO_3$ ceramics with an effective d_{33} in excess of 1200 pC/N.[12] A templated grain growth (TGG) technique was used. In this process, ceramic texture develops as a result of the growth of an ensemble of well-aligned templates into a submicrometer-sized matrix.[13] Templates are usually micrometer-sized single crystal particles, and orient during the green body forming under a shear stress gradient, similar to that present in tape casting. Anisometric particles with high aspect ratios are thus preferred. They are easily obtained in the case of phases with highly anisotropic crystal growth habits, but not in the case of perovskite oxides. This was the reason that in this first attempt, and basically in all that followed, templates were not $Pb(Mg_{1/3}Nb_{2/3})O_3$–$PbTiO_3$ microcrystals, but isostructural particles of simple perovskites such as $BaTiO_3$ or $SrTiO_3$ instead.[14–17]

Best results have been obtained with high aspect ratio platelets obtained by topochemical conversions of Aurivillius particles, and highly textured ceramics have been processed from them by a careful tailoring of the densification and TGG stages.[14,17] However, two-step molten salt processes are required for obtaining the templates, and scalability is not straightforward. Also, and notwithstanding the very good piezoelectric properties reported in the latter works with high-field effective d_{33} of 1500 pC/N and low-field values in resonance of 850 pC/N, the use of low piezoelectric or nonferroelectric templates limits performance.

We have succeeded in processing MPB $Pb(Mg_{1/3}Nb_{2/3})O_3$–$PbTiO_3$ textured ceramics by a novel TGG procedure that involves ceramic-only technology and a single-source powder, which is used for the matrix and also for preparing the templates. These are $Pb(Mg_{1/3}Nb_{2/3})O_3$–$PbTiO_3$ micrometer-sized cubes that are obtained with a range of sizes, either by exaggerated grain growth (EGG) of the nanocrystalline powder, or by TGG of the previous templates in the same powder.[18] We report here main aspects of the processing,

E. Suvaci—contributing editor

Manuscript No. 33156. Received May 6, 2013; approved October 22, 2013.
[†]Author to whom correspondence should be addressed. e-mail: hamorin@icmm.csic.es

along with the microstructure, quantitative preferred orientation, and properties of the materials that show high-field effective piezoelectric coefficients up to 1000 pC/N. This demonstrates the feasibility of obtaining high piezoelectric response in textured ceramics of MPB materials by this novel approach.

II. Experimental Procedure

Powder was nanocrystalline $0.675Pb(Mg_{1/3}Nb_{2/3})O_3$–$0.325PbTiO_3$ with a 2 wt% excess of PbO obtained by mechanochemical activation of the binary oxides in a high-energy planetary mill using tungsten carbide milling media. PbO (99.9%, Aldrich, Steinheim, Germany), MgO (98%, Aldrich), TiO_2 (99.8%, Alfa Aesar, Karlsruhe, Germany), and Nb_2O_5 (99.9%, Aldrich) were used as starting reagents. Details of the procedure and of the mechanisms taking place during the mechanosynthesis were reported elsewhere.[19] This is a powerful technique for the preparation of functional nanocrystalline materials, which allows most known relevant ferroelectric perovskites to be mechanosynthesized.[20–22] Milling conditions were tailored to prepare batches (200 g) with contamination below 50 and 600 ppm of Co and W, respectively.[19] Powder after activation consisted of tight agglomerates of primary nanoparticles, so a deagglomeration treatment was carried out to decrease effective particle size down to the submicrometer range.

$Pb(Mg_{1/3}Nb_{2/3})O_3$–$PbTiO_3$ cubic grains of 10 μm average size were obtained by conventional sintering of the nanocrystalline powder at 1250°C for 1 h in a PbO-oversaturated atmosphere, conditions at which extensive EGG and a degraded microstructure resulted.[23] This was done by placing samples on top of a Pt foil buried in $PbZrO_3$ powder (99%, Aldrich) inside a closed arrangement of two alumina crucibles. Weight losses during this sintering step were about 3 wt %. Cubic grains were separated by leaching the ceramic in acetic acid for 5 min, followed by rinsing in deionised water and high-power ultrasonic processing (Sonics VCX 750; Sonics & Materials Inc., Newtown, CT) in ethanol with a tapered microtip, which resulted in the complete disaggregation of the ceramic grains. The isolated microcrystals were dried and sieved to pass through a 20-μm-mesh sieve. The yield of this template synthesis procedure was 80% of the starting material.

Larger cubes up to 27 μm average size were obtained by TGG processes of the same powder with a 5 wt% of the previous templates under the same extreme conditions (targeting not only full growth, but also microstructure degradation), and separated in the same way described above.[18] The isolated templates were dried and sieved to pass through a 40-μm-mesh sieve while retained on a 20-μm-mesh sieve. The yield of template synthesis procedure in this case was reduced to 50% of the starting material. Optical images of the templates and their size distributions are shown in Fig. 1. Quantitative image analysis was carried out with a computerized system (MIP45; Digital Image Systems S.L., Barcelona, Spain). All thermal treatments were typical ceramic procedures carried out in conventional box furnaces. In addition, cube-shaped microcrystals of 50 μm average size, obtained in this case by crystal growth in PbO flux at high temperatures, were used to validate specific experimental procedures. These have been shown to be suitable for the processing of highly textured ceramics by TGG.[24]

Tape casting was used to obtain green bodies with the cuboidal templates oriented within the matrix. An ethanol-based slurry was developed to avoid the use of highly toxic toluene-based solvents,[25] unlike most of previous works.[12–16,24] This formulation allowed solid loadings up to 30 vol% in the suspensions with Hypermer KD6 (Uniqema, Wirrall, UK) dispersant (1.5 wt%). Poly(vinyl butyral) (Aldrich, St. Louis, MO) binder (5 wt%) and benzylbutyl phthalate (Merck-Schuchardt, Hohenbrunn, Germany) plasticizer (5 wt%) were added, and slurries were obtained after high-energy ball milling for 2 h. Templates (5 wt% on a dry

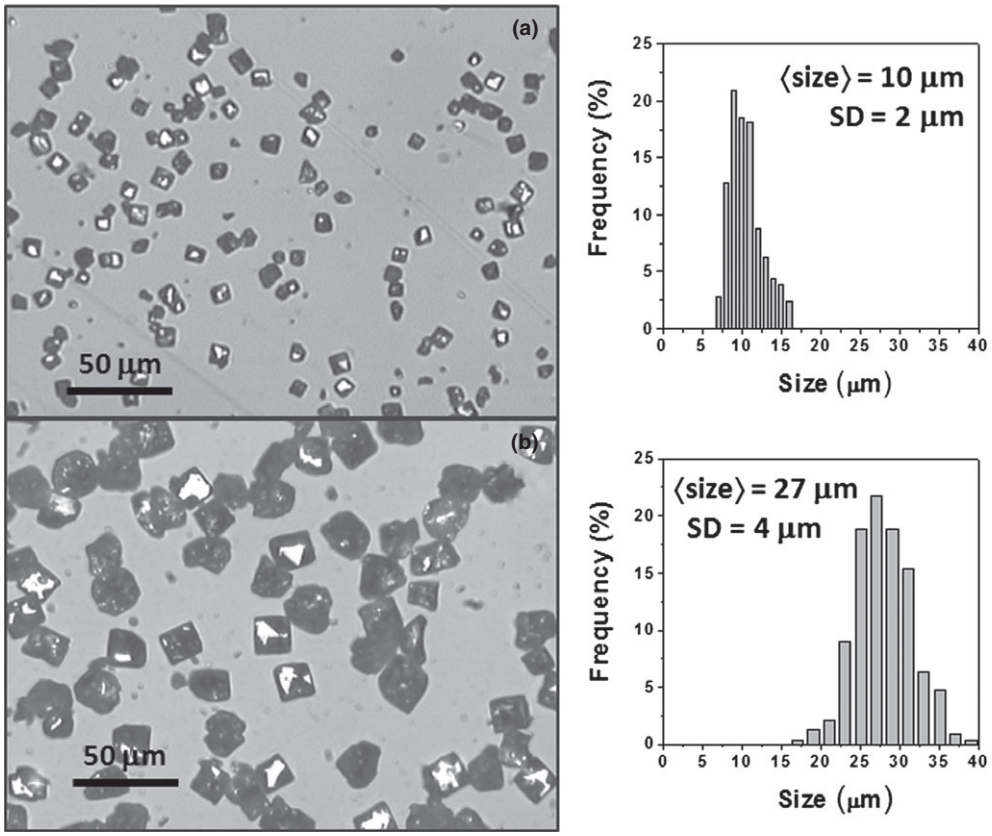

Fig. 1. Optical images of the cubic microcrystals used as templates with (a) 10 μm and (b) 27 μm average sizes and their size distributions.

powder basis) were finally added and stirred for 1 h previous to the tape casting onto silicone-coated Mylar™ (R. E. Mistler, Inc., Yardley, PA). A doctor blade height of 0.1 mm and a casting speed of 2.5 cm/s were selected to obtain a high shear rate of 250 s^{-1}, and thus template alignment within the tapes. After drying for 24 h, tapes with thickness of 35 μm resulted, from which thicker green bodies were prepared by stacking and lamination at room temperature using a uniaxial pressure of 10 MPa. Organics were burned out at 500°C for 2 h, with heating/cooling rates of 0.5°C/min, which are slow enough to prevent cracking and delamination.

Fully dense ceramics (above 99% densification) with submicrometer grain sizes and the templates embedded were obtained by hot-pressing at 850°C for 1 h in air using an alumina die and a uniaxial pressure of 60 MPa. Finally, TGG processes for texture development are triggered with a thermal treatment in a conventional furnace at 1150°C for 10 h with heating/cooling rates of ±5°C/min, also in a PbO-oversaturated atmosphere. In this case, samples were also placed on top of a Pt foil and buried in a coarse particle $Pb(Mg_{1/3}Nb_{2/3})O_3$–$PbTiO_3$ powder with a 7 wt% excess of PbO, inside the closed arrangement of alumina crucibles. Weight losses after this annealing step were lower than 0.5 wt%. Final density was measured by the Archimedes method.

Conventional (θ/2θ geometry) X-ray diffraction (XRD) experiments were carried out using a Siemens D500 (Munich, Germany) diffractometer and CuK_α radiation. A 2θ range from 20° to 70°, in steps of 0.05° with counting time of 5 s/step was scanned, and the Lotgering factor corresponding to the <001>-crystallographic orientation was calculated with the integrated peak intensities. Pole figures were obtained using a Huber 4-circle goniometer (Rimsting, Germany) mounted on a X-ray generator (CuK_α radiation) and equipped with a curved position-sensitive detector (Model CPS-120; Inel, Artenay, France), covering an angle of 120° range in 2θ (angular resolution of 0.03°) for the quantitative texture analysis. X-ray diagrams at different sample orientations were measured varying the tilt angle (χ) between 0° and 60° in steps of 1°, with integration times of 150 s/step.

Ceramic microstructures were characterized with a field-emission gun scanning electron microscope, FEG-SEM (Nova NanoSEM 230 microscope; FEI Company, Hillsboro, OR) on cross sections perpendicular to the casting plane. Sample was prepared by polishing with Al_2O_3 suspensions to 0.1 μm, and by thermal etching at 800°C for 20 min.

Silver electrodes were sintered on the ceramic plates for the electrical and electromechanical characterizations. The temperature dependence of the dielectric permittivity was measured on heating at 1.5°C/min and several frequencies between 100 Hz and 1 MHz using a HP4284A precision inductance-capacitance-resistance Meter (Agilent, Palo Alto, CA). Ferroelectric hysteresis loops were characterized at room temperature by current integration under high-voltage sine waves (0.1 Hz), using a synthesizer/function generator (Model HP3325B; Hewlett-Packard Inc., Palo Alto, CA) and a high-voltage amplifier (Trek Model 10/40A, Medina, NY), whereas charge was measured with a homebuilt charge to voltage converter. Poling was carried out in an oil bath at 150°C under an electric field of 3 kV/mm for 15 min. Strain under the electric field was characterized up to fields of 1 kV/mm. Low-frequency (0.1 Hz) biased (to obtain unipolar driving) sine waves of increasing amplitude were applied.

III. Results and Discussion

Densification and TGG stages were deliberately separated by using a two-step sintering process. It is known that TGG requires a threshold densification to be triggered, and that matrix grain sizes as small as possible are also advantageous.[13] Therefore, the combination of hot pressing and the nanocrystalline powder obtained by mechanosynthesis is especially suitable for obtaining an optimum initial microstructure for the TGG process, that is, ceramics with 99% densification and an average matrix grain size of 150 nm

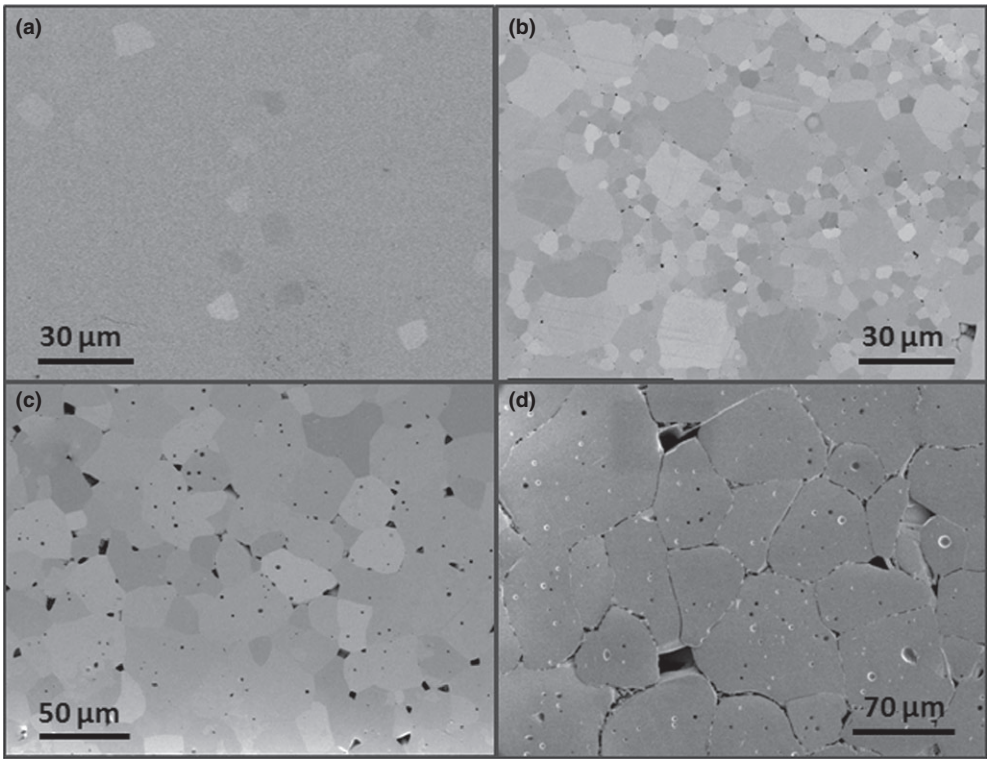

Fig. 2. Field-emission gun scanning electron microscope images of cross sections perpendicular to the casting plane for (a) initial microstructure after hot pressing, (b) partial growth from initial 10 μm templates, (c) full growth from initial 10 μm templates, and (d) full growth from initial 27 μm templates.

were obtained.[26] Figure 2(a) shows the FEG-SEM image of a cross sections perpendicular to the casting plane after hot-pressing stage, in which the templates aligned within a submicrometer-sized matrix, prior triggering TGG phenomena, can be observed.

Texture finally develops during the thermal treatment under controlled PbO atmosphere. Full template growth as well as intermediate states with partial growth were achieved by tailoring the processing parameters with all 10, 27, and 50 μm initial size templates, while maintaining in all cases a high densification (between 96% and 98%). FEG-SEM images of cross sections perpendicular to the casting plane of selected materials are shown in Fig. 2. Templated grains and remnant coarsened matrix can be distinguished for the material arrested at an intermediate stage of the TGG process, as shown in Fig. 2(b) for the ceramic with 10 μm initial size templates. After its completion, a homogeneous microstructure of templated grains results [see Fig. 2(c)] with a final average grain size of 25 μm, determined by quantitative image analysis of more than 100 grown templates. A homogeneous microstructure of large blocky grains was also obtained for the ceramic with the 27 μm initial size templates, as shown in Fig. 2(d), resulting in a final average grain size of 68 μm, also determined by quantitative analysis. Average grain sizes here obtained are comparable to results (i.e., smallest grain size) for textured ceramics obtained using high aspect ratio platelets.[14–17] Even finer microstructures could be achieved by increasing the volume fraction of templates (here only a 5 wt% was used), a strategy that is facilitated by their processing with ceramic-only technologies.

Corresponding XRD diffraction patterns are shown in Fig. 3(a). Note the progressive increase in the intensity of the perovskite (100) and (200) peaks relative to the (110) and (111) ones as the TGG process advances, illustrating the development of texture for the case of the 10 μm initial size templates. Note also the increase in (100) preferred orientation with the size of templates for full-grown materials: the Lotgering factor increases from 0.35 to 0.72 and 0.78 with using initial templates of 10, 27, and 50 μm, respectively. This not only confirms texture development with <001>-preferred orientation perpendicular to the casting plane but also indicates an effect of the template size on their initial orientation during tape casting.

The orientation degree of fully grown materials was further studied by quantitative texture analysis. Pole figures were measured for the 002 Bragg peak, which clearly indicated fiber-type texture perpendicular to the casting plane for all ceramics as expected. Figure 3(b) shows the variation in the diffraction integrated intensity (with the maximum intensity in multiples of a random distribution (MRD) normalized to 1) at increasing tilt angles (χ-scan) for fully grown materials obtained with templates of increasing size. Maximum MRD decreases from 75 to 25, and then to only 2 MRD when using initial templates of 50, 27, and 10 μm, respectively.

It must be noted that χ-scans study the evolution of the integrated intensity of the diffraction peaks at fixed incidence angle; therefore, the same family of crystallographic planes is analyzed. The use of χ-scan is more appropriate than conventional rocking curves for the study of complex diffraction peaks with several contributions, as it is the case for perovskite MPB materials.[27] A March-Dollase texture model was used to fit the measured data using the following equation[28]:

$$F(f,r,\chi) = f\left(r^2\cos^2\chi + \frac{\sin^2\chi}{r}\right)^{-\frac{3}{2}} + (1-f)$$

Strength of the preferred orientation is quantified by the r parameter ($0 < r < 1$), which approaches to zero ($r \to 0$) for fully oriented materials, whereas f stands for the volume fraction of oriented material. The texture parameters

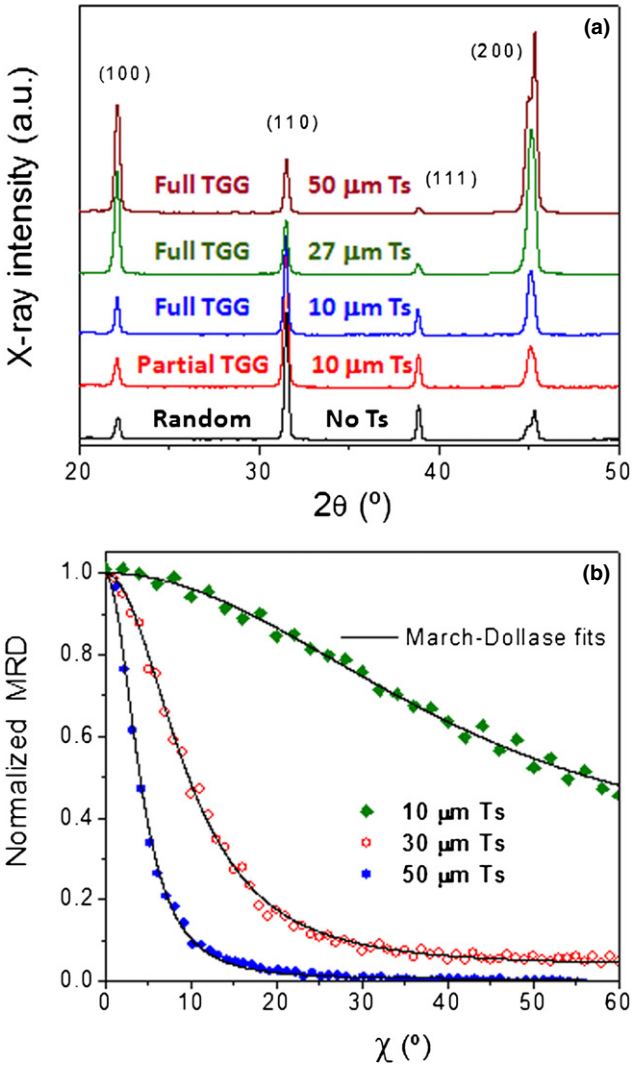

Fig. 3. (a) X-ray diffraction patterns for the randomly oriented and textured ceramics with full and partial growth using initial 10 and 27 μm templates (Ts). (b) χ-scans measurements and fits to the March-Dollase texture model.

obtained for the ceramic processed with 10 μm initial size templates ($r = 0.81$, $f = 0.93$) indicate full growth, but poor preferential orientation defined by the high r value in agreement with the low Lotgering factor. Results for the textured ceramics obtained with 27 μm ($r = 0.32$, $f = 0.83$) and 50 μm initial size templates ($r = 0.21$, $f = 0.70$) indicate high degree of preferred orientation in these latter cases. Indeed, the texture parameters obtained are in the range of best reported for ceramics processed with anisometric templates.[13–17]

The high degree of preferred orientation achieved with cuboidal templates is somewhat surprising and does not follow from simple mathematical models of shear alignment. It cannot be said at this point whether templates align under the shear gradient or they simply settled in the suspension with flat <001> faces in contact with the casting surface. However, results show that the initial template size is crucial on their initial orientation after the tape casting, and experiments (not shown here) with blade height of 0.2 mm and maintaining the same shear rate results in lower degrees of orientation with all templates. This suggest that a given relation between template size and blade height seems to be required to achieve high degree of preferred orientation when cuboidal templates are used, indicating a role of the shear gradient.

The temperature dependence of the relative dielectric permittivity at several frequencies is shown in Fig. 4. Results for textured ceramics obtained with the initial 10 and 27 μm

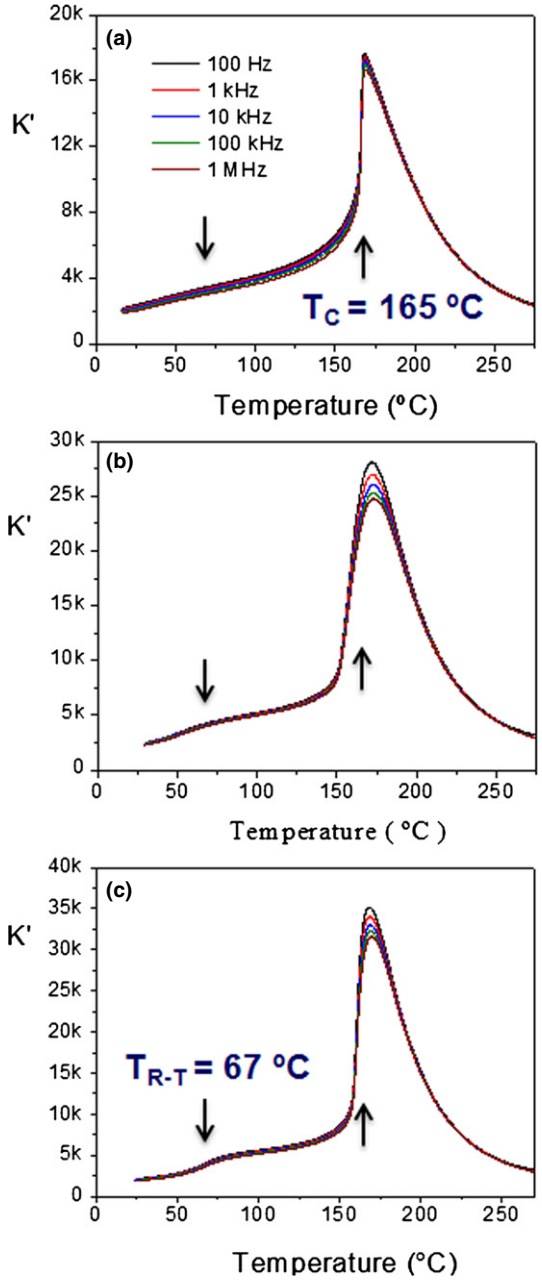

Fig. 4. Temperature dependence of the dielectric permittivity at several frequencies (arrows indicate transition temperature) for the (a) conventional ceramic, (b) fully grown ceramic with initial 10 μm templates, and (c) fully grown ceramic with initial 27 μm templates.

templates (Figs. 4(b) and (c), respectively), and thus with increasing degree of texture are compared with those for a conventional coarse grained, nonoriented material [Fig. 4(a)]. This system, and specifically this composition at MPB presents a relaxor to ferroelectric phase transition, and thus the dispersive maximum is rather associated with the dynamics of the relaxor state than with the phase transition itself,[29] which takes place at the inflection point marked with an arrow in the figure. Note the transition to occur at practically the same temperature; $T_C \sim 165$°C, for the textured materials and for the randomly oriented ceramic. Nonnegligible transition shifts toward room temperature have been reported for textured ceramics obtained using $SrTiO_3$ or $Na_{1/2}Bi_{1/2}TiO_3$–$PbTiO_3$ templates with a significant impact in the properties.[14–17] Note also the high value of the maximum permittivity up to 35.000 for the textured ceramics. This favorably compares with previous results for textured ceramics using isostructural templates with maximum permittivity

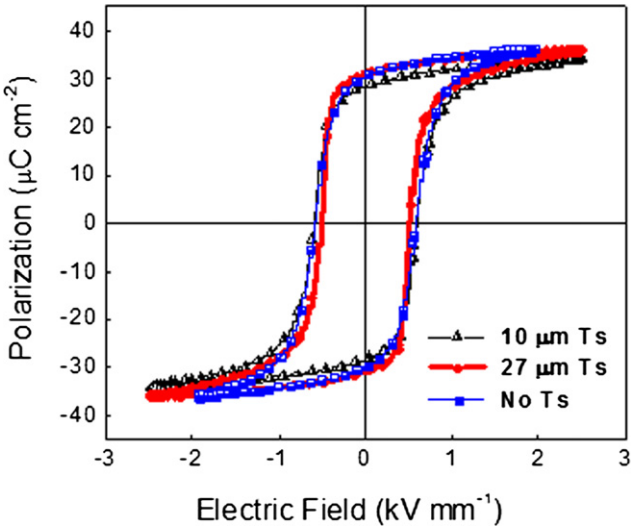

Fig. 5. Ferroelectric hysteresis loops under saturation for a conventional ceramic and the fully grown ceramics with initial 10 and 27 μm templates.

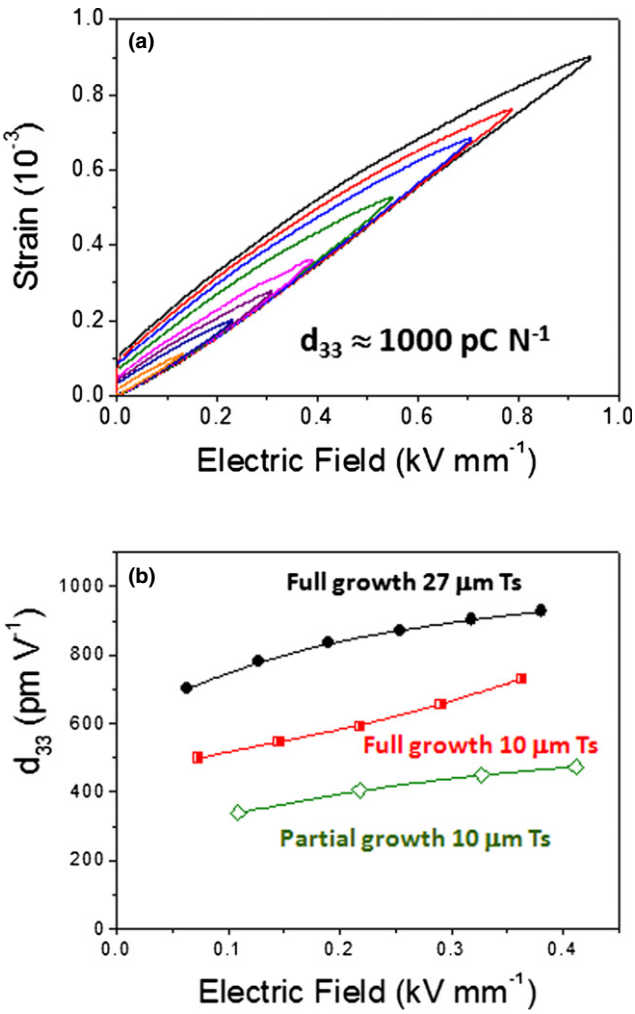

Fig. 6. (a) Strain under increasing electric fields for the fully grown ceramics with initial 27 μm templates, and (b) effective d_{33} piezoelectric coefficients for fully grown ceramics with initial 10 and 27 μm templates and partially grown ceramic with initial 10 μm templates.

below 25.000, and highlights the advantages of using Pb$(Mg_{1/3}Nb_{2/3})O_3$–$PbTiO_3$ templates instead of high aspect ratio particles of simple perovskites. Indeed, permittivity data

for the ceramic obtained with the initial 27 μm templates closely resembles that for (001)-cut single crystals of the same composition.[30] It is also remarkable the sharpness of the dielectric anomaly associated with the rhombohedral to tetragonal phase transition at $T_{R-T} \sim 67°C$.

Ferroelectric hysteresis loops are given in Fig. 5. The squareness of the loop with very high remnant polarization ($P_r \sim 30\ \mu C/cm^2$) and low coercitivity ($E_c \sim 0.5$ kV/mm) for the textured ceramic obtained with the initial 27 μm templates are comparable to that of single crystals.[30] Therefore, it can be concluded that textured ceramics with electrical properties approaching those of single crystals have been successfully processed by the novel approach.

Finally, the electromechanical properties are summarized in Fig. 6. Strain under increasing electric fields is shown in Fig. 6(a) for the fully textured ceramic obtained with initial 27 μm templates as an example. Results for the different materials are compared in Fig. 6(b), where the effective d_{33} piezoelectric coefficient is given as a function of the applied electric field. There is a clear effect of the degree of texture on the maximum strain, and thus on the effective d_{33} that increases up to a value that approaches 1000 pC/N (to 1 kV/mm). This effective d_{33} is comparable to those previously reported for Pb$(Mg_{1/3}Nb_{2/3})O_3$–$PbTiO_3$ textured ceramics when an excess of PbO was introduced for promoting TGG; for example, 990 pC/N (to 1 kV/mm) for a material with Lotgering factor of 0.75, processed with high aspect ratio (above 5) $SrTiO_3$ platelets, which grow in the presence of a 3 wt% excess of PbO,[14] or 880 pC/N (to 3 kV/mm) for 0.68PMN–0.32PT textured ceramics with a Lotgering factor as high as 0.99, this time prepared with analogous $BaTiO_3$ templates and a 1.5 wt% excess of PbO.[15]

Further research must be directed toward removing the hot-pressing step in a first stage and the excess of PbO in the matrix in a second one. These objectives have already been achieved with platelets prepared by topochemical reactions. Full densification (above 99%) with limited grain growth prior to TGG was obtained by carrying out a presintering step under a controlled PbO-deficient atmosphere.[17] Also, an excess of PbO in the matrix can be avoided by carrying out the following TGG thermal treatment in a PbO-oversaturated atmosphere under tailored conditions. The liquid phase in this case is provided by the PbO vapor by condensation and permeation across the ceramic. Textured ceramics with a densification level above 99% and a Lotgering factor of 0.87 were recently reported by this processing.[17] Although the sintering and TGG behaviors of the nanocrystalline powder obtained by mechanosynthesis are different, similar results could be expected by its tailoring.

IV. Conclusions

This study demonstrates the feasibility of processing Pb$(Mg_{1/3}Nb_{2/3})O_3$–$PbTiO_3$ textured ceramics from cuboidal templates of the same phase, by using a single-source nanocrystalline powder and ceramic-only technologies. The materials present high density and a homogenous microstructure with an average grain size that can be controlled with the template size down to a value of 25 μm. High degree of preferred orientation was achieved with cuboidal templates of 27 μm initial sizes. Ferroelectric properties approaching those of single crystals and effective d_{33} up to 1000 pC/N have been obtained, figures that are liable of improvement by tailoring the TGG process. This demonstrates the feasibility of obtaining high piezoelectric response textured ceramics by this novel TGG approach, a main line of research in piezoelectric ceramics.

Acknowledgments

The authors acknowledge involvement of Prof. Marija Kosec, who passed away in December 2012. Her support and input was essential to success. Research was funded by Spanish former MICINN (now MINECO) through project MAT2011-23709. H. A. thanks support by the "Ramón y Cajal" program, and H. U. that by the Slovenian Research Agency (SRA, project J2-3633) and CoE NAMASTE. D.C. acknowledges specific financial support for the X-ray instrument for quantitative texture analysis by Conseil Régional de Basse Normandie. Authors are especially grateful to Ms. Tamara Molina at ICV-CSIC and Silvo Drnovšek at JSI for the technical assistance in the processing.

References

[1]S. R. Anton and H. A. Sodano, "A Review of Power Harvesting Using Piezoelectric Materials (2003–2006)," *Smart Mater. Struct.*, **16** [3] R1–21 (2007).

[2]S. G. Kim, S. Priya, and I. Kanno, "Piezoelectric MEMS for Energy Harvesting," *MRS Bull.*, **37**, 1039–50 (2012).

[3]C. W. Nan, M. I. Bichurin, S. Dong, D. Viehland, and G. Srinivasan, "Multiferroic Magnetoelectric Composites: Historical Perspective, Status, and Future Directions," *J. Appl. Phys.*, **103** [3] 031101, 35pp (2008).

[4]Y. Yan, K.-H. Cho, and S. Priya, "Templated Grain Growth of <001>-Textured $0.675Pb(Mg_{1/3}Nb_{2/3})O_3$–$0.325PbTiO_3$ Piezoelectric Ceramics for Magnetic Field Sensors," *J. Am. Ceram. Soc.*, **94** [6] 1784–93 (2011).

[5]N. Setter, *Piezoelectric Materials in Devices*. Ceramics Laboratory EPFL, Lausanne, 2002.

[6]D. Damjanovic, "Comments on Origins of Enhanced Piezoelectric Properties in Ferroelectrics," *IEEE Trans. Ultrason. Ferroelectr. Freq. Control*, **56** [8] 1574–85 (2009).

[7]B. Noheda, J. A. Gonzalo, L. E. Cross, R. Guo, S. E. Park, D. E. Cox, and G. Shirane, "Tetragonal-to-Monoclinic Phase Transition in a Ferroelectric Perovskite: The Structure of $PbZr_{0.52}Ti_{0.48}O_3$," *Phys. Rev. B*, **61** [13] 8687–95 (2000).

[8]H. X. Fu and R. E. Cohen, "Polarization Rotation Mechanism for Ultrahigh Electromechanical Response in Single-Crystal Piezoelectrics," *Nature*, **403**, 281–3 (2000).

[9]S. E. Park and T. R. Shrout, "Ultrahigh Strain and Piezoelectric Behavior in Relaxor Based Ferroelectric Single Crystals," *J. Appl. Phys.*, **82** [4] 1804–11 (1997).

[10]K. Uchino, "Materials Issues in Design and Performance of Piezoelectric Actuators: An Overview," *Acta Mater.*, **46** [11] 3745–53 (1998).

[11]S. J. Zhang and F. Li, "High Performance Ferroelectric Relaxor–$PbTiO_3$ Single Crystals: Status and Perspective," *J. Appl. Phys.*, **111** [3] 031301, 50pp (2012).

[12]E. M. Sabolsky, A. R. James, S. Kwon, S. Trolier-McKinstry, and G. L. Messing, "Piezoelectric Properties of <001> Textured $Pb(Mg_{1/3}Nb_{2/3})O_3$–$PbTiO_3$ Ceramics," *Appl. Phys. Lett.*, **78** [17] 2551–3 (2001).

[13]G. L. Messing, S. Trolier-McKinstry, E. M. Sabolsky, C. Duran, S. Kwon, B. Brahmaroutu, P. Park, H. Yilmaz, P. W. Rehrig, K. B. Eitel, E. Suvaci, M. M. Seabaugh, and K. S. Oh, "Templated Grain Growth of Textured Piezoelectric Ceramics," *Crit. Rev. Solid State Mater. Sci.*, **29**, 45–96 (2004).

[14]S. Kwon, E. M. Sabolsky, G. L. Messing, and S. Trolier-McKinstry, "High Strain, ⟨001⟩ Textured $0.675Pb(Mg_{1/3}Nb_{2/3})O_3$–$0.325PbTiO_3$ Ceramics: Templated Grain Growth and Piezoelectric Properties," *J. Am. Ceram. Soc.*, **88** [2] 312–7 (2005).

[15]T. Richter, S. Denneler, C. Schuh, E. Suvaci, and R. Moos, "Textured PMN–PT and PMN–PZT," *J. Am. Ceram. Soc.*, **91** [3] 929–33 (2008).

[16]K. H. Brosnan, S. F. Poterala, R. J. Meyer, S. Misture, and G. L. Messing, "Templated Grain Growth of ⟨001⟩ Textured PMN–28PT Using SrTiO3 Templates," *J. Am. Ceram. Soc.*, **92** [S1] S133–9 (2009).

[17]S. F. Poterala, S. Trolier-McKinstry, R. J. Meyer Jr., and G. L. Messing, "Processing, Texture Quality, and Piezoelectric Properties of $\langle 001\rangle_C$ Textured (1-x)$Pb(Mg_{1/3}Nb_{2/3})TiO_3$–$XPbTiO_3$ Ceramics," *J. Appl. Phys.*, **110**, 014105, 8pp (2011).

[18]H. Amorín, J. Ricote, J. Holc, M. Kosec, and M. Algueró, "Homogeneous Templated Grain Growth of $0.65Pb(Mg_{1/3}Nb_{2/3})O_3$–$0.35PbTiO_3$ From Nanocrystalline Powders Obtained by Mechanochemical Activation," *J. Eur. Ceram. Soc.*, **28** [14] 2755–63 (2008).

[19]D. Kuscer, J. Holc, and M. Kosec, "Formation of $0.65Pb(Mg_{1/3}Nb_{2/3})O_3$–$0.35PbTiO_3$ Using a High-Energy Milling Process," *J. Am. Ceram. Soc.*, **90** [1] 29–35 (2007).

[20]J. Wang, D. M. Wan, J. M. Xue, and W. B. Ng, "Mechanochemical Synthesis of $0.9Pb(Mg_{1/3}Nb_{2/3})O_3$–$0.1PbTiO_3$ From Mixed Oxides," *Adv. Mater.*, **11** [3] 210–3 (1999).

[21]M. Algueró, J. Ricote, T. Hungría, and A. Castro, "High-Sensitivity Piezoelectric, Low-Tolerance-Factor Perovskites by Mechanosynthesis," *Chem. Mater.*, **19**, 4982–90 (2007).

[22]M. Algueró, P. Ramos, R. Jiménez, H. Amorín, E. Vila, and A. Castro, "High Temperature Piezoelectric $BiScO_3$–$PbTiO_3$ Synthesized by Mechanochemical Methods," *Acta Mater.*, **60**, 1174–83 (2012).

[23]M. Algueró, A. Moure, L. Pardo, J. Holc, and M. Kosec, "Processing by Mechanosynthesis and Properties of Piezoelectric $Pb(Mg_{1/3}Nb_{2/3})O_3$–$PbTiO_3$ With Different Compositions," *Acta Mater.*, **54** [2] 501–11 (2006).

[24]M. Pham-Thi, H. Hemery, O. Durand, and H. Dammak, "Orientation Distribution and Fiber Texture of Highly Oriented Piezoceramics: $(1-x)PbMg_{1/3}Nb_{2/3}O_3$–$XPbTiO_3$ System," *Jpn. J. Appl. Phys.*, **43** [12] 8190–4 (2004).

[25]H. Amorín, I. Santacruz, J. Holc, M. P. Thi, M. Kosec, R. Moreno, and M. Alguero, "Tape-Casting Performance of Ethanol Slurries for the Processing of Textured PMN-PT Ceramics from Nanocrystalline Powder," *J. Am. Ceram. Soc.*, **92** [5] 996–1001 (2009).

[26]H. Amorín, J. Ricote, R. Jiménez, J. Holc, M. Kosec, and M. Algueró, "Submicron and Nanostructured $0.8Pb(Mg_{1/3}Nb_{2/3})O_3$–$0.2PbTiO_3$ Ceramics by Hot Pressing of Nanocrystalline Powders," *Scripta Mater.*, **58**, 755–8 (2008).

[27]H. Amorín, D. Chateigner, J. Holc, M. Kosec, M. Algueró, and J. Ricote, "Combined Structural and Quantitative Texture Analysis of Morphotropic Phase Boundary $Pb(Mg_{1/3}Nb_{2/3})O_3$–$PbTiO_3$ Ceramics," *J. Am. Ceram. Soc.*, **95** [9] 2965–71 (2012).

[28]W. A. Dollase, "Correction of Intensities for Preferred Orientation in Powder Diffractometry – Application of the March Model," *J. Appl. Crystallogr.*, **19**, 267–72 (1986).

[29]V. Bovtun, S. Kamba, S. Veljko, D. Nuzhnyy, J. Kroupa, M. Savinov, P. Vanek, J. Petzelt, J. Holc, M. Kosec, H. Amorín, and M. Algueró, "Broadband Dielectric Spectroscopy of Phonons and Polar Nanoclusters in $PbMg_{1/3}Nb_{2/3}O_3$–35%$PbTiO_3$ Ceramics: Grain Size Effects," *Phys. Rev. B*, **79**, 104111, 12pp (2009).

[30]Z. G. Ye, *Handbook of Advanced Dielectric, Piezoelectric and Ferroelectric Materials: Synthesis, Properties and Applications*. Woodhead Publishing Limited, Cambridge, 2008. □